Advances in Science and Technology Research Journal

*Advances in Science and Technology Research Journal*, 2025, 19(12), 219–237
https://doi.org/10.12913/22998624/209900
ISSN 2299-8624, License CC-BY 4.0

Received: 2025.07.28
Accepted: 2025.10.01
Published: 2025.11.01

# The new protective anti-graffiti coatings for railway vehicles – manufacturing technology and properties

Norbert Radek[1*], Ewa Kozień[2], Łukasz Pasieczyński[3], Łukasz Jan Orman[1], Marek Kozień[4]

[1] Faculty of Mechatronics and Mechanical Engineering, Kielce University of Technology, Al. 1000-lecia P. P. 7, 25-314 Kielce, Poland
[2] College of Management and Quality Sciences, Cracow University of Economics, ul. Rakowicka 27, 31-510 Cracow, Poland
[3] Firma Handlowa Barwa Jarosław Czajkowski, ul. Warkocz 3-5, 25-253 Kielce, Poland
[4] Faculty of Environmental Engineering, Geomatics and Renewable Energy, Kielce University of Technology, Al. 1000-lecia P. P. 7, 25-314 Kielce, Poland
[5] Faculty of Mechanical Engineering, Cracow University of Technology, Al. Jana Pawła II 37, 31-864 Cracow, Poland
* Corresponding author's e-mail: norrad@tu.kielce.pl

## ABSTRACT

Due to the costs, the unexpected appearance of graffiti on rail vehicles and the need to remove it is an increasingly serious problem for rail carriers. The use of anti-graffiti protective coatings by rail companies is becoming more and more common. These coatings must meet appropriate quality requirements, in particular regarding their mechanical properties and features, such as roughness, adhesion. The use of anti-graffiti coatings is also associated with the technology of their production and removal, taking into account the problem of environmental impact and costs. Some of the anti-graffiti coating systems were tested and compared. Anti-graffiti coating systems were characterized by low parameters of the geometric structure of the surface and good adhesion. Moreover, they had good mechanical properties and were free of structural defects as pores or microcracks. Anti-graffiti paint systems were characterized by hydrophobicity, which helps reduce the adhesion of undesirable substances on their surfaces. Also discussed are various aspects of the costs incurred by railway companies due to the existence and removal of graffiti from passenger cars. Economic analyses included data from Polish and Spanish national and regional railway companies.

**Keywords:** anti-graffiti coatings, properties, cost analysis, railway transport, sustainable development.

## INTRODUCTION

Among problems, the incidence of which is systematically increasing, and in particular applies to rail transport is the removal of the consequences of vandalism, which is the problem of destruction of train cars, especially passenger trainsets, by graffiti painting, which has become a challenge for many railway companies in Europe, including Poland, in the 21st century. In the paper [1] the problem of costs incurred by rail carriers in the world (in Germany, Spain, Belgium, the Netherlands, Australia) is discussed. Some of the economic and management aspects that throw quantitative and cost dimensions of the problem are briefly presented in a separate section 2. The analysis of costs of anti-graffiti removal is not the main research axis of the article, but it is important in the overall view of the research problem of graffiti removal, just as, for example, in the paper [2] the economic analysis performed also had the character of extending the research from the point of view of practical applications. Graffiti found on railcars violates the exterior aesthetics of trains

and lowers the element of distinction of the network operator and the type of vehicle. Nowadays, during vehicle production, rolling stock manufacturers are required to apply an anti-graffiti coating in addition to painting the exterior plating. Polish rolling stock manufacturer PESA has been using such coatings since 2004 [3]. The paint coating of Elf2 railbuses ordered for Małopolska in PESA is mandatory to be covered with a special layer that prevents the application of graffiti and is supposed to fulfill its properties for the shortest period of 10 years [4]. It is important that the coating is made in accordance with the technological and production process of the vehicle manufacturer. Vehicle manufacturers indicate that the parameters of the paint coating are maintained when the anti-graffiti coating is painted ten times and the graffiti paint is removed using the appropriate procedure with dedicated agents. They further state that the amount of cleaning of the graffiti surface, as well as the impact of graffiti, i.e. the degree of damage to the paint coating, depends primarily on the type of paint and graffiti coating materials, the length of time the graffiti remains on the vehicle paint surface, from the application until the graffiti surface is washed off, and the atmospheric conditions, ambient temperature, humidity, sunshine, precipitation affecting the applied graffiti. All repair, renovation work is carried out in the repair hall, maintaining appropriate temperatures, in pollution-free conditions. The materials used to repair paint coatings must meet the conditions in accordance with the manufacturer's technology. Anti-graffiti coatings are being modified by manufacturers on an ongoing basis, following the fact that graffiti paints are also becoming more aggressive. The company BARWA has developed a new family of anti-graffiti coatings. The paper presents analyses concerning the study of the required properties that these coatings should meet.

The properties of the surface layer affect the service life of machinery and equipment. The surface fundamentally affects the performance of objects and products. A number of physicochemical phenomena such as chemical catalysis, corrosion, wear (abrasive, adhesive, abrasive-adhesive, erosive, cavitation, fatigue), adhesion, adsorption (physical and chemical), flotation, depend on and take place on the surface of the material or with its participation [5–7]. Coatings are simultaneously affected by various types of factors: thermal and corrosive (alkalis, acids, and salts), moisture, and solar radiation in the form of destructive UV radiation, whose influence on the destruction process of coatings is synergistic [8, 9]. The impact of operating environment factors has a significant effect on the condition of the surface of polymer coatings. As a result of adsorption of aggressive substances on the surface of coatings, as well as the impact of ultraviolet radiation, intensive chemical and physical destruction of the surface of coatings occurs, primarily deteriorating their decorative properties [10–13]. The penetration of aggressive media into the interior of polymer coatings can also cause swelling and blistering, as a result of the accumulation of media near the substrate and due to the development of subsurface corrosion [14]. The effects of the influence of aggressive substances increase if the polymeric material has also been subjected to the influence of other operating factors, such as heat, mechanical loads, including the impact of erosion particles (hail, sand, clods of earth, stones) [15]. From the moment the application process is completed, the coating is exposed to destructive operating factors. One of the most dangerous factors destroying polymer coatings are aggressive media (acid rain, brine, battery acid), destroying their chemical structure through leaching, hydrolysis, or oxidation [16–19]. In the initial stage of destruction, there is a deterioration of the decorative properties of coatings (dulling, color change, loss of gloss), while in its final stage, the aggressive media migrating deep into the coating cause corrosion wear of the substrate [20]. When aqueous solutions of sodium chloride affect the paint coating, the first stage of its destruction process is the formation of conductive paths (capillaries), which allow direct access of chloride ions to the surface of the metal substrate [17, 18, 20]. The rate of diffusion of aggressive media in polymer coatings decreases as the number of layers increases. Anticorrosion properties of organic coatings is presented in [21]. The influence of the surface texture of dedicated composite for wet painting, on durability of gloss parameters and colour [22]. Various strategies and methods are considered to eliminate graffiti from rail vehicles. In article [1] is presented the original ultra-freezing air projection method. While in the article [23] the environmentally safe graffiti remover is proposed.

Initially, paint coating systems were designed to protect the surface of steel from aggressive external agents and to impart color. With the help of paint coatings, special effects and properties began to be imparted to the vehicles to which these

systems were applied. One such system with special properties is the protective anti-graffiti coating system [24–26]. When we talk about a protective coating system that includes a clear anti-graffiti coating, we are talking about a coating that gives the ability to easily remove unwanted subsequent layers of paint without damaging the original paint layer. This can be achieved by using a highly chemically and mechanically resistant coating or by giving it properties that reduce the adhesion of subsequent layers. Reduced adhesion means that it is easier to remove anything that is found on the surface of the structure: dust, acidic or alkaline deposits, but also graffiti paint. The use of special anti-graffiti coating systems helps reduce vandalism on rolling stock and speeds up the process of removing damage caused by graffiti. For this purpose, less aggressive cleaning agents should be used, which ultimately contributes to environmental protection and reduces the losses that are incurred as a result of railway vehicles (wagons) downtime.

This paper presents the results of tests on selected operational properties of anti-graffiti coating systems developed by BARWA. Current research includes measurements of surface geometric structure, adhesion, surface free energy, hardness, and microstructure analysis. Attention is paid to parameters relevant to the operation of railway wagons. An attempt was also made to estimate the costs of anti-graffiti removal incurred by railway carriers.

## COSTS OF ANTI-GRAFFITI REMOVAL

When analyzing the economic aspects of destroying train depots by painting graffiti, the problem should be looked at holistically, taking into account the technological aspect discussed earlier, but also the ecological, social, managerial, as well as legal aspects.

Most of discussed above involve large additional costs for rail companies. For example, at the moment, the cost of repairing a damaged EN57-type depot alone is in the range of 6000–8000 EUR. The cost of removing graffiti from railroad cars includes: material costs, energy costs, direct labor costs. In the case of damage to the paint coating on the vehicle, taking into account the mechanical damage to the paintwork caused by repeated acts of vandalism (several times applied and removed layers of pseudo-graffiti with violation and mechanical destruction of both the paint and the performed undercoat), estimated in terms of the required materials as well as labor intensity in accordance with the current processes of repair and restoration of paint, converted for one square meter of the repaired area is about 200 EUR net. This cost is an estimate, it does not take into account the significant costs of taking the vehicle out of service and stopping it to perform graffiti removal activities, but essentially takes into account the following scope of work:

- Verification, determination of the area of repair, taping and protection of the bordering surfaces;
- Repairing the occurring mechanical damage, scratches, degreasing, sanding, polishing and dust removal, and making the repair layer;
- Selecting the color scheme, taking into account the shades of the adjacent surfaces of the base paints, and carrying out the renovation with the base paints for the given paint surface, taking into account the drying and evaporation times;
- Restoration of damaged inscriptions, descriptions, decals;
- Applying a new layer of anti-graffiti clearcoat to the entire repaired surface;
- Removal of protections, polishing, and washing of repaired surfaces.

To illustrate the problem, data from selected years relating to the Polish National Railway Company (PKP), Polish regional railway companies (Mazovia Railways, Silesian Railways, Małopolska Railways) and the national rail company in Spain - Renfe Operadora (RENFE La Red Nacional de Ferrocarriles Españoles) - are summarized. Table 1 summarizes the costs incurred by the carriers in selected years for the specified operations related to the removal of graffiti from railcars. Table 2 summarizes the areas of railcars damaged by graffiti, while Table 3 lists the number of acts of vandalism.

The upward trend in the cost, area and number of cases of graffiti removal for the Malopolska Railways in 2021–2023 is shown in the graphs in Figure 1. There is an increase in the number of cases by 28% over the two years analyzed, as well as a 150% increase in the area subjected to renovation (graffiti removal). On the other hand, the cost of renovation has increased more than five times. This means, the need for widespread use of atygraffiti coatings and rapid removal of graffiti.

**Table 1.** Costs incurred by railway companies (in thousand PLN)

| Year | Company | Activity | Cost, kPLN | Source |
|---|---|---|---|---|
| 2001 | PKP Railways | Removal of graffiti | 227 | [24] |
| 2017 | Mazovia Railways | Removal of graffiti | 1 700 | [25] |
| 2018 | Silesian Railways | Removal of graffiti | 60 | [25] |
| 2022 | RENFE Railways | Total graffiti costs | 100 000 | [26] |
| 2021 | Malopolska Railways | Removal of graffiti | 37 | own |
| 2022 | Malopolska Railways | Removal of graffiti | 121 | own |
| 2023 | Malopolska Railways | Removal of graffiti | 200 | own |

**Table 2.** The area of the surface of graffiti being removed (in thousands of square meters)

| Year | Company | Area, km$^2$ | Source |
|---|---|---|---|
| 2017 | Mazovia Railways | 11 | [25] |
| 2018 | Mazovia Railways | 8 | [25] |
| 2018 | RENFE Railways | 80 | [26] |
| 2021 | Malopolska Railways | 0.4 | own |
| 2022 | Malopolska Railways | 0.9 | own |
| 2023 | Malopolska Railways | 1 | own |

**Table 3.** Total number of graffiti acts of vandalism

| Year | Company | Number | Source |
|---|---|---|---|
| 2018 | Silesian Railways | 40 | [25] |
| 2022 | RENFE Railways | 3559 | [26] |
| 2021 | Malopolska Railways | 39 | own |
| 2022 | Malopolska Railways | 44 | own |
| 2023 | Malopolska Railways | 50 | own |

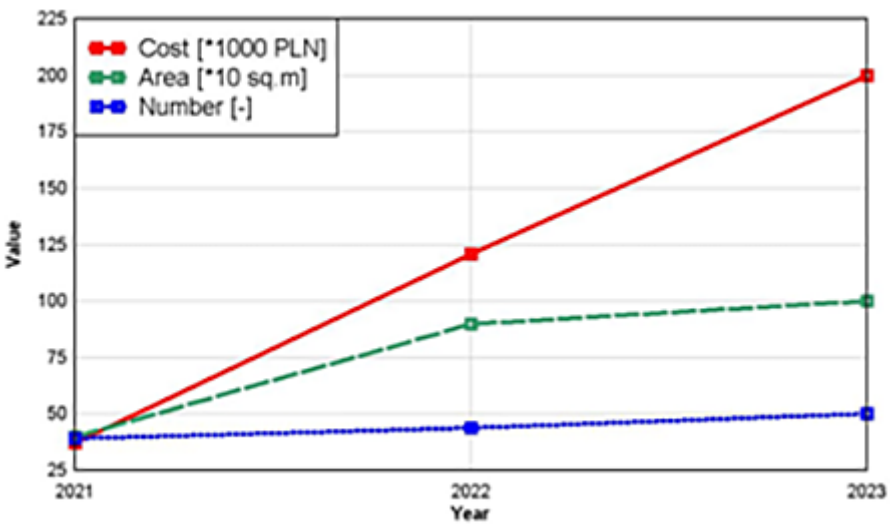


**Figure 1.** Trend in costs, areas and number of cases for the Malopolska Railways

It is worth noting the difficulties faced by preventive measures. Despite the costs incurred for the system of monitoring and protection of rolling stock in 2022, the Spanish carrier RENFE recorded 3559 incursions by graffiti artists into railroad areas, and only in 729 cases was it possible to prevent vandalism. Some of the apprehended vandals have been punished in court proceedings. The painting

of trains also affects subway depots. For example, in February 2023, in the morning hours at a subway station, vandals painted a subway depot by blocking the depot‘s movement with an emergency brake beforehand [30], in August 2023, at night at a subway station, a group of masked vandals painted a subway train by stopping its movement with an emergency brake beforehand [31], and in December 2023, at night at a subway station, 10 vandals painted a subway train almost its entire length in less than five minutes [32].

An analysis of the cost of removing graffiti from railway vehicles or wagons requires investment in an effective system for monitoring and protecting oil rolling stock, which must be combined with a civic-minded public. On the other hand, the failure to take systemic and preventive measures, as well as the failure to reduce the scale of graffiti vandalism, will increase the cost of removing graffiti from train depots following an increase in the price of anti-graffiti paints and labor costs.

## MATERIALS AND METHODS

### Protective coatings

A coating system with special properties is a protective anti-graffiti coating system. The main purpose of using this coating is to protect the surface of the structure from corrosion. The use of joint compound makes it possible to improve the shape of the structure resulting from heat transport during welding work in the production process. To give the aesthetics desired by the customer - in the form of color, gloss or special decorative effects (hammer effect, crease effect). The result is the protection of the vehicle from the end user in the form of a specialized anti-graffiti layer. The protective system fulfills its function if it adheres tightly to the vehicle surface and maintains its continuity. When graffiti paint appears on the protective coating, physical and, in some cases, chemical changes occur in the coating. By physical changes we mean the diffusion of solvents and the carrier medium included in graffiti varnishes. Such a coating, due to interaction with chemical solvents such as acetone, xylene, mesylene, butyl acetate, ethyl acetate and solvent mixtures (toluene solvent, white spirit, nitro), can be destroyed. In the first stage, solvents can migrate deep into the coating and cause it to soften. In subsequent stages, such a coating may become fluffed up, cracked and even delaminated. The damage will mainly depend on the aggressive components of the graffiti paint. In addition, the conditions in which the vehicle is located, such as high sunlight resulting in the heating of the vehicle, combined with aggressive solvents in the graffiti paint can have a devastating effect on the protective coating. Another key parameter is time, in order not to allow graffiti to contact the protective coating for too long, the composition is immediately taken out of service and directed to washing. Contaminants that have more firmly “bonded” to the surface of the clearcoat can be removed chemically or mechanically, while being aware of the gradual damage to the clearcoat. Such actions can lead to a reduction in the thickness of the clearcoat (with a dry film thickness of about 40–60 μm). After several repetitions of such a process, the basecoat may be exposed. The entire system will then be significantly weakened, which will directly affect its aesthetics and the component’s susceptibility to corrosion. This can lead to a situation where it will be necessary to carry out refinishing ahead of schedule, which will generate unnecessary costs. It seems reasonable to use such a clear coat to protect the system from external influences as much as possible. The clearcoat that finishes the system should also exhibit special characteristics, such as reduced adhesion of subsequent layers and their eventual easy removal.

### Anti-graffiti coatings laboratory tests

The way the paint system is made has a major impact on the vehicle’s service life. The performance tests compared three paint systems based on anti-graffiti coatings from PPG (the world’s leading paint manufacturer) with a paint system that included BO100-AGR paint coating (developed in the laboratory of Firma Handlowa Barwa Jarosław Czajkowski). The following anti-graffiti coating systems were considered in laboratory tests: XPC 60012, XPC 60011, XPC 60036 and BO100-AGR with the properties given in Table 4.

Each coating system consisted of an epoxy anti-corrosion primer, polyester putty, polyurethane filler, an aesthetic base coat and a colourless anti-graffiti varnish applied to an alloy steel core. The compositions of the individual layers were not given due to the trade secrets of the manufacturers (PPG and Firma Handlowa Barwa Jarosław Czajkowski).

**Table 4.** Physical parameters of the coating systems used in tests

| Material | Mass density, kg/m$^3$ | Weight proportion |
|---|---|---|
| XPC60011 | 990 | 1:1 |
| XPC60012 | 980 | 3:1 |
| XPC60036 | 1010 | 2:1 |
| BO100-AGR | 1020 | 2:1 |

In order to compare different anti-graffiti coating systems with each other and determine their suitability, the performance properties of the coating system (mechanical properties, physical-chemical properties) were selected, which translate into an assessment of their service life and cost of performance. The test specimens were made of the S355 alloy steel. The surface preparation and coating (painting) procedure was strictly defined and repeatable for all samples and coatings applied. The procedure was described in detail in [33].

Based on our research, the following parameters for the application of on anti-graffiti coating were assumed:

- application technique: pneumatic spray,
- application: four layers,
- surface temperature: 21–23 °C,
- operating pressure: 0.20–0.22 MPa,
- evaporation time between layers: 20 minutes,
- evaporation before baking: 20 minutes,
- annealing temperature: 50 °C,
- annealing time: 60 minutes,
- thickness of dry film: 40–50 µm.

The remaining layers were applied in accordance with the technical data sheets recommended by the manufacturers

### *Microstructural analysis*

Samples for metallographic testing were cut using an ISOMET cutting machine. The cut specimens were then embedded in BUEHLER KonductoMet thermosetting conductive resin using a BUEHLER SimplyMet 3000 inlay press. The metallographic specimens were ground on a BUEHLER MetaServ 250 grinder on water papers with grain gradations from 80 to 2500, each time changing the angle by 90° to the direction of the scratches from the previous paper gradation. Polishing of the specimens was carried out on a BUEHLER EcoMet 250 grinder-polisher with pneumatically adjustable pressure and speed. The specimens were polished on MicroDiamant Mambo cloth in MicroDiamant O.P.S suspension 0.05 µm. The metallographic specimens prepared in this way were subjected to microscopic observations. A JEOL type JSM-7100F field emission scanning electron microscope (SEM) was used to study the microstructure.

The photograph (Figure 2) shows an example of the microstructure of the BO100-AGR anti-graffiti coating system. Based on the results, the minimum thickness of the anti-graffiti coating was about 42 µm, while the maximum thickness was about 43 µm.

SEM analysis showed that the thickness of the basecoat layer was between 18–19 µm. The undercoat layer had a thickness in the range of about 50 µm to 55 µm. The layer with putty had the greatest thickness of about 2210 ÷ 2250 µm. Clear boundaries between the individual layers can be seen (Figure 2). In addition, Figure 2 shows a clear boundary between the paint layers and the putty. We can also observe that the paint layers are free of pores and micro-cracks. Analyzing the morphology of the other anti-graffiti coating systems XPC 60011, XPC 60036, BO100-AGR, it was found that the thicknesses of the individual layers are comparable to the thicknesses of the layers of the XPC 60012 anti-graffiti coating system. The thickness of the anti-graffiti coating systems produced ranged from about 2300 to about 2400 µm.

### *Measurement of surface free energy*

So far, a method for direct measurement of surface free energy (SFE) has not been developed. For this purpose, an indirect method is used, based on measuring the angle of wetting of surfaces by reference liquids, and then using mathematical models, the surface free energy is calculated [34, 35].

The determination of the wetting angle of the surface of structural materials was used according to a method based on the geometry of the droplet. The surface of the droplet is most often shaped like a bowl, and then the wetting angle is calculated from measuring (h) the height of the bowl and (r) the radius of the droplet's contact area. The

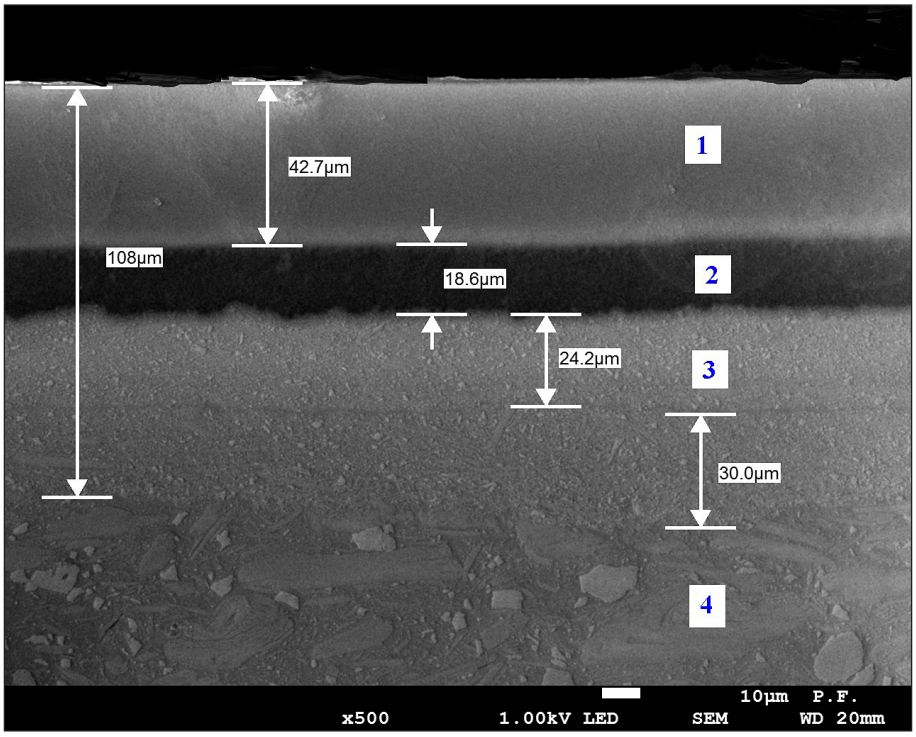


**Figure 2.** SEM image of the polished cross-section through an anti-graffiti BO100-AGR coating system on steel substrate: 1 – anti–graffiti layer, 2 – base layer, 3 – undercoat layer, 4 – putty

canopy height is given by the formula h = R(1-cosθ), and the surface contact radius r = Rsinθ. From these relationships, we get Equation 1 [1]:

$$\Theta = \frac{2h}{r} \tag{1}$$

where: $\theta$ – angle of wetting of the surface, $h$ – height of the canopy, $r$ – the radius of the droplet contact surface.

The value of the surface free energy of structural materials is determined indirectly using the measurement of wetting angles with selected measuring fluids. Distilled water and diiodomethane (DIM) were used as measuring fluids for measuring the wetting angle. A stereoscopic microscope with a camera and MicroScan v 1.3 software was used to observe the droplets and measure the wetting angle.

The following values of the surface free energy constants of the measuring fluids and their polar and dispersive components were adopted: $g_w$ = 72.8 mJ/m$^2$, $g_{pw}$ = 51.0 mJ/m$^2$, $g_{dw}$ = 21.8 mJ/m$^2$, $g_d$ = 50.8 mJ/m$^2$, $g_{pd}$ = 2.3 mJ/m$^2$, $g_{dd}$ = 48.5 mJ/m$^2$. The measuring liquid was applied to the test surface using a micropipette with a fixed volume of 5 µl.

The surfaces of the polymers that were studied are polar, so in this case the SFE calculated by the Zisman method is not appropriate. The Owens-Wendt method is commonly used to determine the surface free energy of composite materials in which the surface free energy is assumed to be the sum of two components: dispersive and polar (2) [1]:

$$\gamma_s = \gamma_s^d + \gamma_s^p \tag{2}$$

where: $\gamma_s$ – surface free energy, $\gamma_s^d$ – dispersive component of surface free energy, $\gamma_s^p$ – the polar component of the surface free energy.

The measurement series consisted of measurements of the wetting angle of ten successively injected drops of liquid onto the surface of the paint system. The measured wetting angle of the coating system by a given liquid was used to calculate the surface free energy. The same methodology was used to test each anti-graffiti coating system. Taking ten measurements for each coating system allowed the test results to be averaged.

Figure 3 compares the surface free energy of the anti-graffiti coating systems tested. To achieve reduced contaminant adhesion of the protective layer, the free surface energy is sought to be minimized. The lowest surface free energy values were shown by the XPC60011

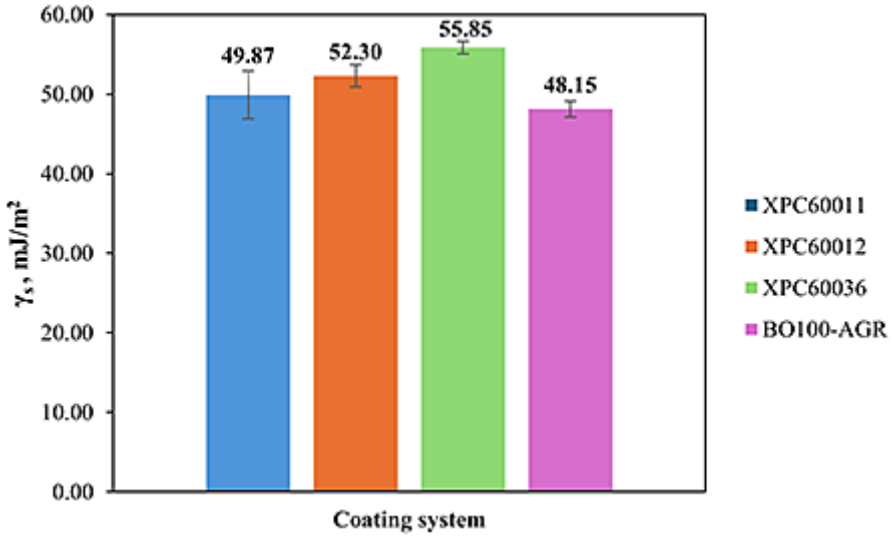


**Figure 3.** Comparison of the total surface free energy of the tested systems anti-graffiti coatings

and BO100-AGR coating systems. From the point of view of rolling stock and anti-graffiti protection, these two systems had the desired properties. The aforementioned anti-graffiti paint systems were characterized by hydrophobicity, which is conducive to reducing the adhesion of undesirable substances on their surfaces. However, it should be borne in mind that graffiti paints consist of various resins, fillers, pigments and additives, so synergistic interactions may occur, making it difficult to predict the exact mechanism of interaction between hydrophilic and hydrophobic surfaces. As the of the material increases (smaller wetting angle), more work needs to be done to disconnect the surface of the coating system from contaminants formed on the surface. The more hydrophobic the material was, the greater the wetting angle, and the smaller the adhesion work.

Figure 4 shows the surface free energy of the anti-graffiti coating systems tested, divided into dispersive and polar components. It is noteworthy that the dispersion component contributed the most to the increase in the total SFE value. The XPC 60011, XPC60012 and XPC60036 paint systems were characterized by a similar value of the dispersion component. However, in the case of the XPC 60011 coating system, the reduced adhesion of graffiti varnishes was achieved by reducing the polar component of SFE.

The polar component is the sum of components derived from interactions between molecules, including polar, inductive, hydrogen, acid-base interactions. Dispersive interactions, on the other hand, represent the dispersive component of surface free energy. Modification of the developed BO100-AGR coating system leads to a reduction in the value of surface free energy. This is primarily associated with a decrease in its dispersion component, compared to the other coating systems studied. By chemically modifying the SEP between contacting phases, larger wetting angles can be achieved with unwanted substances. On the other hand, by modifying the surface of the material with a chemical substance, the chemical composition, structure, or roughness of the surface layer is changed, resulting in changes in interfacial interactions. For these reasons, only results obtained by the same method and using the same measuring fluids can be the subject of comparative analyses of SFE values.

Further research work should determine whether SFE changes during operation or remains constant. Also of interest is the change in surface free energy after successive cycles of both vehicle washing and graffiti paint washing. However, when conducting studies to determine the degree of degradation and kinetics of change under the influence of external factors, it should be borne in mind that simulating the external environment yields approximate results, and verification of the error is only possible by conducting independent tests on a real sample.

The example is proof of the great importance of SFE in the process of creating polyurethane protective coatings that meet the requirements of modern materials engineering.

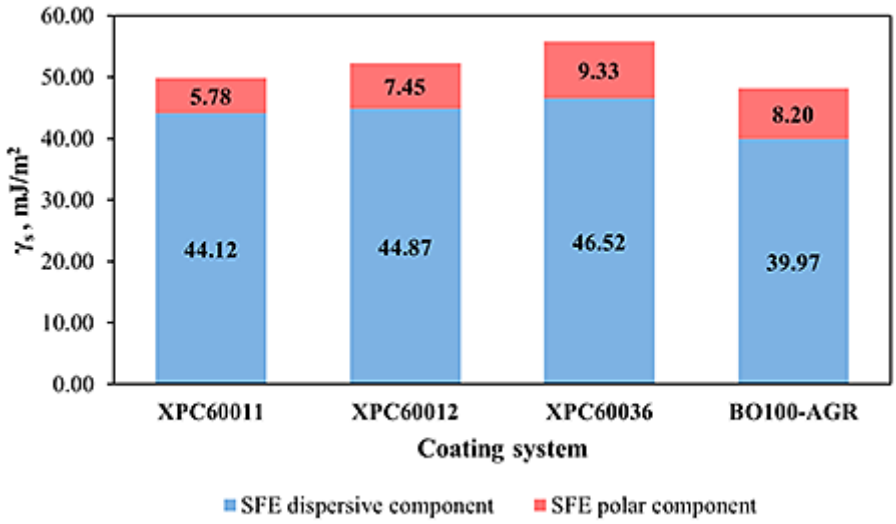


**Figure 4.** Comparison of the components of the total surface energy of the tested systems anti-graffiti coatings

Based on the obtained results statistical analysis of surface free energy of anti-graffiti coating systems The obtained results of performed in 6 replication measurements results are grouped into 4 groups reflecting the adopted technological systems. The analysis covered 3 observed values: total surface free energy (TSFE), dispersive component of surface free energy (DC-TSFE) and polar component of surface free energy (PC-TSFE).

When comparing the mean values, the homogeneity of variance was checked using Leven's test. In the case of non-contradiction with the assumption of homogeneity of means, the classical ANOVA analysis of variance was performed with simultaneous determination of homogeneous groups using the Tukey test. In the case of rejection of the hypothesis of homogeneity of means, the test of their equality was performed using the Welch test with simultaneous determination of homogeneous groups using the Games-Howell method.

The results of detailed statistical analyses performed for total surface free energy (TSFE), dispersive component of total surface free energy (DC-TSFE) and polar component of total surface free energy (PC-TSFE) are presented below.

## Total surface free energy (TSFE)

Descriptive statistics for total surface free energy TSFE are presented in Table 5.

Leven's test of homogeneity of variance was performed, which rejected ($p < 0.001$) the hypothesis of equality of variances. An attempt to perform the Box-Cox transformation showed the optimal value of the parameter $\lambda > 5$, which means that it is impossible to achieve variance stabilization in this way. Therefore, an assessment of the equality of mean values was performed using the Welch method, which rejected ($p < 0.001$) the hypothesis of equality of all mean values. Figure 5 presents a box plot of individual groups. Next, possible homogeneous groups were identified, i.e. sets of measured values that are statistically indistinguishable. Identification of homogeneous groups using the Games-Howell method showed the existence of 3 homogeneous groups, 2 of which over-lapped each other (Table 6).

## Dispersive component of total surface free energy (DC-TSFE)

Descriptive statistics for the dispersive component of the total surface free energy DC-TSFE are presented in Table 7.

Leven's test of homogeneity of variance was performed, which not rejected the hypothesis of equality of variances ($p = 0.41$). Therefore, an assessment of the equality of mean values was performed using the classic ANOVA method, which rejected ($p < 0.001$) the hypothesis of equality of all mean values. Figure 6 presents a box plot of individual groups. Next, possible homogeneous groups were identified, i.e. sets of measured values that are statistically indistinguishable. Identification of homogeneous groups using the Tukey Pairwise Comparison method showed the existence of 3 non-overlapped homogeneous groups (Table 8).

**Table 5.** Descriptive statistics for total surface free energy TSFE

| Coating system | Mean | SE Mean | StDev | Min. | Median | Max. |
|---|---|---|---|---|---|---|
| BO-100AGR | 48.15 | 0.28 | 0.69 | 47.2 | 48.15 | 49.2 |
| XPC60011 | 49.87 | 1.28 | 3.14 | 46.9 | 49.55 | 53.4 |
| XPC60012 | 52.30 | 0.36 | 0.87 | 51.0 | 52.40 | 53.3 |
| XPC60036 | 55.85 | 0.23 | 0.55 | 55.1 | 55.85 | 56.6 |

**Table 6.** Total surface free energy TSFE homogeneous groups (95% confidence level)

| Coating system | N | Mean | Grouping | | |
|---|---|---|---|---|---|
| XPC60036 | 6 | 55.9 | A | | |
| XPC60012 | 6 | 52.3 | | B | |
| XPC60011 | 6 | 49.9 | | B | C |
| BO-100AGR | 6 | 48.2 | | | C |

**Table 7.** Descriptive statistics for the dispersive component of the total surface free energy DC-TSFE

| Coating system | Mean | SE Mean | StDev | Min. | Median | Max. |
|---|---|---|---|---|---|---|
| BO-100AGR | 39.97 | 0.13 | 0.33 | 39.5 | 40.00 | 40.3 |
| XPC60011 | 44.12 | 0.25 | 0.61 | 43.6 | 43.95 | 45.3 |
| XPC60012 | 44.87 | 0.34 | 0.84 | 44.0 | 44.85 | 46.3 |
| XPC60036 | 46.52 | 0.15 | 0.37 | 46.1 | 46.45 | 47.0 |

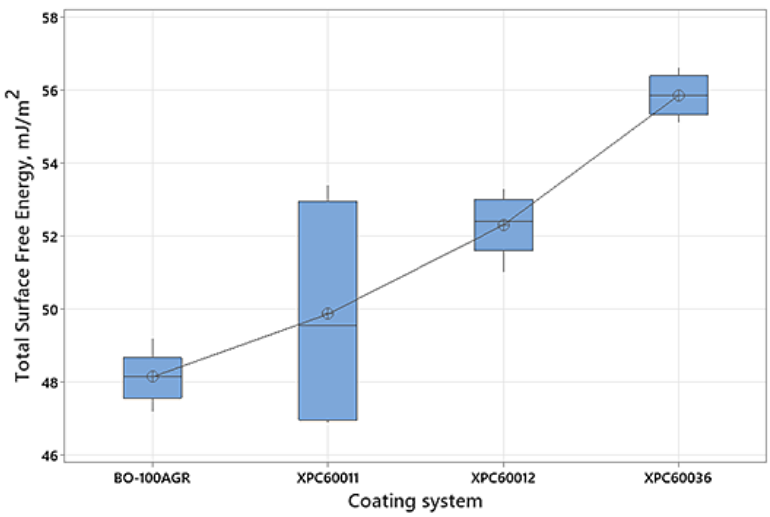


**Figure 5.** Distribution of total surface free energy TSFE values

## Polar component of total surface free energy (PC-TSFE)

Descriptive statistics for the polar component of the total surface free energy PC-TSFE are presented in Table 9.

Leven's test of homogeneity of variance was performed, which rejected ($p < 0.001$) the hypothesis of equality of variances. An attempt to perform the Box-Cox transformation showed the optimal value of the parameter $\lambda = 4$, however, after its execution, the Leven test still indicated the lack of homogeneity of variance ($p = 0.005$). Therefore, an assessment of the equality of mean values was performed using the Welch method, which rejected ($p < 0.001$) the hypothesis of equality of all mean values. Figure 7 presents a box plot of individual groups. Next, possible homogeneous groups were identified, i.e. sets of measured values that are

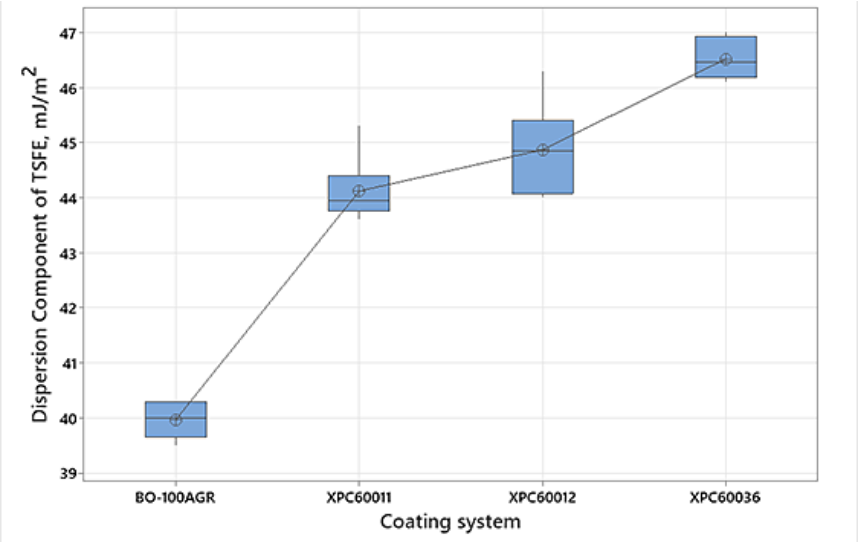


**Figure 6.** Distribution of the dispersive component of the total surface free energy DC-TSFE values

**Table 8.** Dispersion component of the total surface free energy DC-TSFE homogeneous groups (95% confidence level)

| Coating system | N | Mean | Grouping | | |
|---|---|---|---|---|---|
| XPC60036 | 6 | 46.5 | A | | |
| XPC60012 | 6 | 44.9 | | B | |
| XPC60011 | 6 | 44.1 | | B | |
| BO-100AGR | 6 | 40.0 | | | C |

**Table 9.** Descriptive statistics for the polar component of the total surface free energy PC-TSFE

| Coating system | Mean | SE Mean | StDev | Min. | Median | Max. |
|---|---|---|---|---|---|---|
| BO-100AGR | 8.20 | 0.30 | 0.73 | 6.9 | 8.25 | 9.1 |
| XPC60011 | 5.78 | 1.17 | 2.88 | 3.1 | 5.65 | 8.8 |
| XPC60012 | 7.45 | 0.35 | 0.85 | 5.9 | 7.75 | 8.2 |
| XPC60036 | 9.33 | 0.13 | 0.31 | 8.9 | 9.35 | 9.8 |

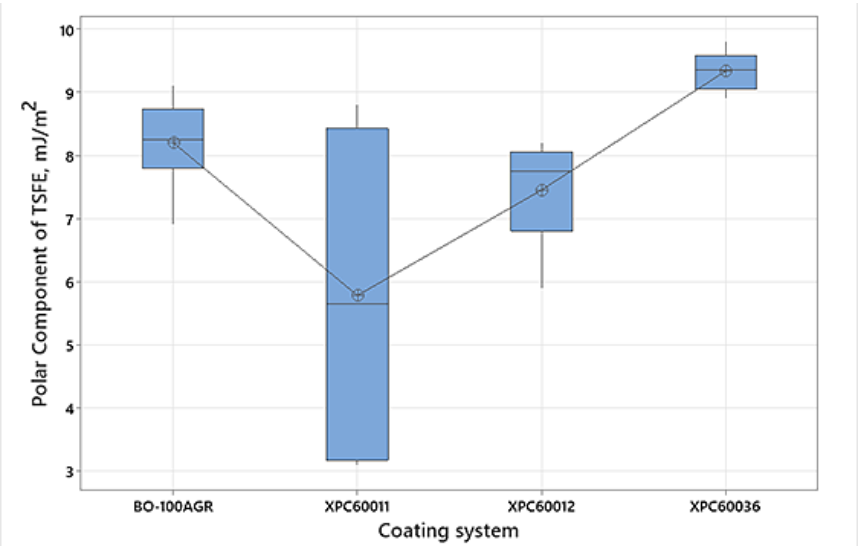


**Figure 7.** Distribution of the dispersive component of the total surface free energy DC-TSFE values

statistically indistinguishable. Identification of homogeneous groups using the Games-Howell method showed the existence of 2 homogeneous non overlapped groups (Table 10).

## Measurements of the surface geometric structure

The geometric structure of the surface has a significant impact on many processes occurring in the surface layer and is one of the most important factors determining its quality values. It has a significant impact on the operational properties of machine elements, which include, for example: friction conditions on the contact surfaces of the mating elements, contact stresses, fatigue strength, corrosion resistance, tightness of connections, surface thermal radiation and magnetic properties. The problems of measurement methods and the assessment of surface roughness and waviness are discussed in the works [36–38]. The measuring devices and method of test speciment preparation are described in detail in the paper [33].

Comparison of surface roughness is visualized for selected single measurements for the tested anti-graffiti coatings are shown in Figure 8. The anti-graffiti coating systems had average *Sa* values ranging from 6.4 nm to 24.6 nm. The substrate material (after grinding) to which the multi-layer coating systems were applied had Sa = 1234.5–1863.2 nm. As a result of applying the anti-graffiti coatings, the parameters of the surface geometric structure were significantly reduced.

### *Adhesion*

The adhesion results of the coating systems were similar to each other. From the test results obtained, the XPC 60011 anti-graffiti coating system (2.28 MPa) had the highest average adhesion value. The XPC 60012 paint system (2.18 MPa) characterized by the lowest average adhesion value had a 5% lower adhesion, compared to the XPC 60011 coating system.

The adhesion results obtained were characterized by low standard deviation values, indicating the high repeatability of the test performed. Measurement of adhesion by the peel method after the test cycle in the aging chambers was also performed. The obtained adhesion results along with the standard deviation are summarized in Table 11. Figure 9 shows the sample after the adhesion test.

Significantly greater differences in adhesion values were observed between the tested systems after exposing the samples to condensation moisture. The XPC 60011 anti-graffiti coating system had the highest adhesion value of 2.23 MPa, compared to the system with the lowest adhesion value of 2.02 MPa (BO100-AGR). The percent change in adhesion value from the initial value before exposure was also calculated. In this case, the XPC 60011 coating system also had the smallest change, with a reduced adhesion of 2.34%. Such a small change can be considered a measurement error. On the other hand, the largest change in adhesion was observed for the XPC60036 anti-graffiti coating system, a reduction in adhesion of 9.73% compared to the initial value was recorded.

## Nanohardness

The production of coatings with the required micromechanical properties is a major research challenge. In the production process, it is necessary to determine the controlled parameters and

**Table 10.** Polar component of the total surface free energy PC-TSFE homogeneous groups (95% confidence level)

| Coating system | N | Mean | Grouping | |
|---|---|---|---|---|
| XPC60036 | 6 | 9.33 | A | |
| XPC60012 | 6 | 8.20 | | B |
| XPC60011 | 6 | 7.45 | | B |
| BO-100AGR | 6 | 5.78 | | B |

**Table 11.** Values of chosen parameters of adhesiveness (MPa) obtained by the peel-off method

| Coating system | Average value | Standard deviation | Range |
|---|---|---|---|
| XPC 60011 | 2.28 | 0.14 | 0.38 |
| XPC 60012 | 2.18 | 0.08 | 0.25 |
| XPC 60036 | 2.24 | 0.07 | 0.19 |
| BO100-AGR | 2.22 | 0.07 | 0.18 |

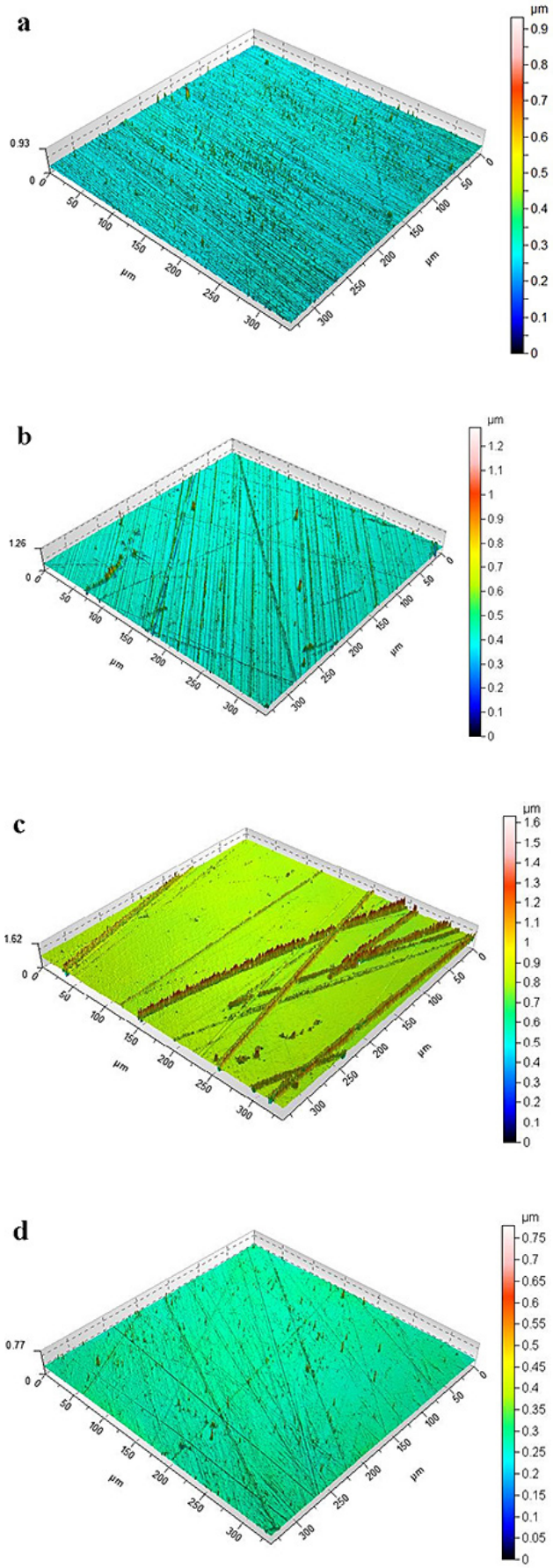


**Figure 8.** Surface roughness for the anti-graffiti coatings: a) XPC 60012, b) XPC 60036, c) XPC 60011, d) BO100-AGR

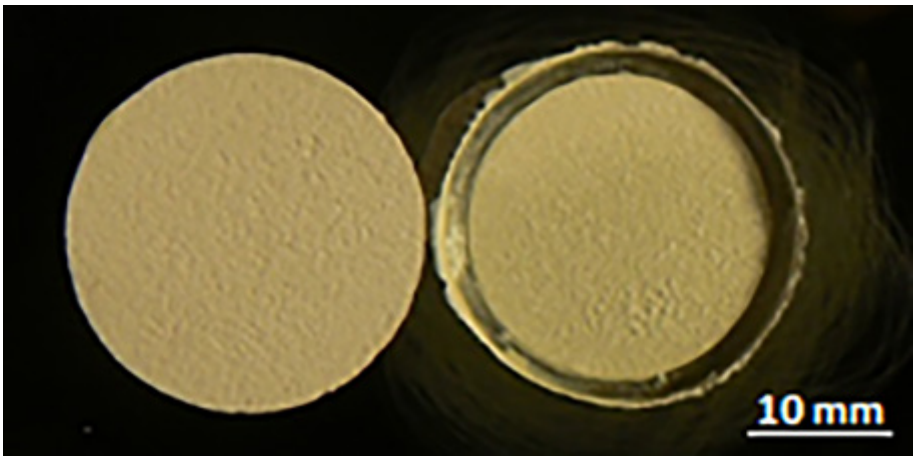


**Figure 9.** View of sample after adhesion test of XPC 60012 coating system

properties that we expect from the resulting coating. The multitude of controlled parameters and their values means that a large number of combinations affects high costs. In our case, we investigated the nanohardness and the modulus of longitudinal elasticity (Young's modulus) of anti-graffiti coating systems.

Nanohardness and Young's modulus measurements were performed using a NANOVEA nanohardness tester. The nanohardness tester consists of a Berkovich indenter, an optical microscope and a motorized stage in the X and Y axes. Precise determination of the measurement location is possible thanks to the sample positioning system with an accuracy of 1 μm. Additionally, which is particularly important when testing thin layers, the force is measured with an accuracy of 0.01 mN, and the indenter penetration is up to 10 nm. The device allows for measurements using an indentation force from 1 mN to 400 mN.

Nanohardness and Young's modulus of the tested samples were measured on the surface in the anti-graffiti paint layer and on the cross-sections of the coating system (mixed sections) in each layer, i.e. anti-graffiti layer, base layer, primer layer, filler and substrate material (S355 steel). The tests were performed with the following parameters: linear load, max. load 3 mN, load and unload speed 40 mN/min and the break time between subsequent load and unload cycles 3 s. The average values of nanohardness and Young's modulus were determined based on 10 measurements.

Nanohardness was determined as the indenter penetration depth, while the modulus of elasticity was determined by the slope of the unloading curve. The results of nanohardness and Young's modulus measurements are presented in Table 12.

The highest nanohardness was found in the S355 alloy steel. which was 10.6 GPa. The Young's modulus was also the highest for the S355 steel. at 124 GPa. Analyzing the data in Table 10 it can be concluded that all anti-graffiti paint coatings had similar nanohardness values. The nanohardness measured on the surface of the anti-graffiti coatings was in the range of 0.229 GPa to 0.265 GPa.

A similar analogy can be observed when analyzing the values of Young's moduli for the tested anti-graffiti paint layers (Table 12). The highest value of the longitudinal modulus of elasticity was found in the BO100-AGR anti-graffiti paint layer compared to the other three anti-graffiti paint layers. The Young's modulus measured on the surface of the BO100-AGR layer was 2.900 GPa. The XPC 60012, XPC 60011, XPC 60036 paint layers had Young's modulus values in the range of 2.700–2.843 GPa (measured on the surface of the coating). The greater elasticity of the BO100-AGR anti-graffiti top layer compared to the other three anti-graffiti paint layers may result from the additives that make up its chemical composition. Example views of the indenter impressions are shown in Figure 10.

The obtained results of nanohardness and Young's modulus measurements show that the anti-graffiti paint coatings were characterized by high homogeneity and the absence of defects in their structure, e.g. the absence of pores and microcracks.

### *Hardness*

The hardness measurement consisted of measuring the damping time of the pendulum according to the standard PN-EN ISO 1522 [39]. The sample was placed on the table of the device. and

**Table 12.** Average values of nanohardness and modulus of elasticity in the anti-graffiti coating measured on the surface

| Materials | Nanohardness, GPa | Young's modulus, GPa |
|---|---|---|
| XPC 60012 | 0.23 ± 0.01 | 2.70 ± 0.05 |
| BO100-AGR | 0.26 ± 0.01 | 2.90 ± 0.02 |
| XPC 60011 | 0.27 ± 0.01 | 2.84 ± 0.04 |
| XPC 60036 | 0.26 ± 0.01 | 2.84 ± 0.03 |
| Steel S355 | 10.60 ± 0.70 | 124.00 ± 5.30 |

then the pendulum legs were gently positioned on its surface. A Koenig pendulum was used in the tests. During the measurement the number of oscillations over time with damped vibrations of the pendulum from the initial yaw angle of 6 deg to a final angle of 3 deg from vertical was counted. The photocell in the device was responsible for the correct number of counts. The number of oscillations was converted to pendulum damping time. In a properly calibrated device using a Koenig pendulum, time of one oscillation should be about 1.4 s. The measurement was carried out six times on each sample in order to average the hardness according to the thickness of the coating. The principle of the measurement was to change the friction surface between the coating under test and the pendulum legs, which translates into the damping time of the pendulum. Coatings with lower hardness more easily yield to the weight of the pendulum, whose legs penetrate the coating more deeply, resulting in an increase in the friction surface. Hardness measurements were also made after exposing the samples to aging chambers. The initial results and the results obtained after testing in the salt chamber and humidity chamber are shown in Table 13. The results shown are the averages of 6 measurements. The method is characterized by high repeatability and reproducibility of results.

Individual results may change slightly in cyclic tests. Therefore. a relative hardness was introduced, which is calculated by dividing the oscillation value of the sample by the oscillation value of the calibration. The preceding calibration measurement ended with a value of 180 oscillations. Relative hardness values are also shown in Table 11 for comparison of each system. The XPC 60012 anti-graffiti coating system had the lowest oscillation damping value (83.7 s), compared to the BO100-AGR coating system, with the highest oscillation damping time (120.8 s). An increase in the hardness of the anti-graffiti coating systems was observed after aging tests in the salt chamber and humidity chamber. All tested coating systems were characterized by high damping times falling within the range of 132–140 s. When measured after the salt chamber tests. the largest increase (by 162% of the initial value) in damping time was obtained for the XPC 60012 coating system, while the XPC 60011 anti-graffiti coating system had the highest hardness corresponding to 140 s of test duration. After the test in the humidity chamber, the paint systems also had high and similar pendulum damping time values (146–150 s). The XPC 60012 anti-graffiti coating system had the highest hardness after completed exposure to moisture, while the lowest average result was completed for the XPC 60036 coating system. Aging tests were conducted at elevated temperatures (313 K). The test conditions in the aging chambers may have accelerated the evaporation of solvents that remained in the individual layers after the conditioning period. During the drying process of the anti-corrosion primer, about 95% of the solvents evaporate from the primer layer, with the remaining 5% evaporating over a period of up to 3 weeks. Applying another layer of the coating system over the anticorrosive primer will extend this time significantly. The remaining small amount of solvent in each layer of the system translates into hardness by the pendulum damping method. Placing the samples in an aging chamber at an elevated temperature for the duration of the hardness test accelerated the migration of the remaining solvents in the system affecting its hardness.

## DISCUSSION

These studies indicate that modification of the surface layer to reduce its surface free energy contributes to obtaining protective coating systems for special applications. Coating systems prepared in this way are characterized by reduced adhesion of unwanted substances on their surface.

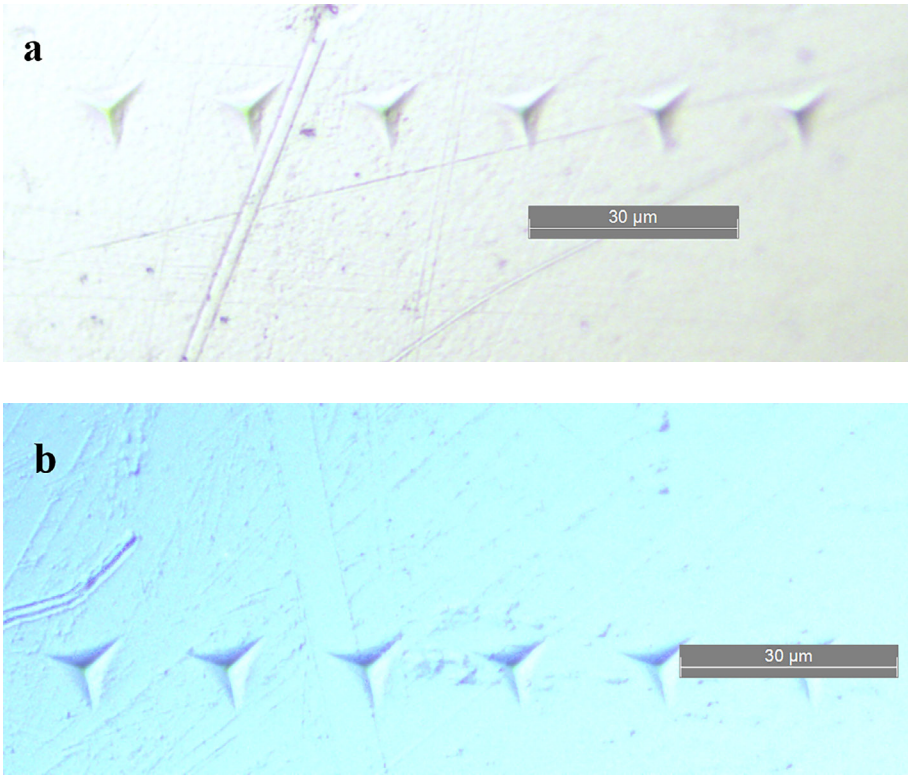


**Figure 10.** Indentation marks during nanohardness measurements on the surface of anti-graffiti paint coating: a) BO100-AGR, b) XPC 60036

**Table 13.** Hardness measurement results according to PN-EN ISO 1522 - Koenig pendulum

| Coating system | Damping time, s | Relative hardness | Damping time – salt, s | Damping time – humidity, s |
|---|---|---|---|---|
| XPC 60011 | 95.2 | 0.4 | 140.0 | 146.7 |
| XPC 60012 | 83.7 | 0.3 | 135.0 | 150.9 |
| XPC 60036 | 109.8 | 0.4 | 132.2 | 145.9 |
| BO100-AGR | 120.8 | 0.5 | 134.4 | 147.8 |

Unwanted substances on the surface layer of a coating system are various types of operational dirt and man-made contaminants such as graffiti. Reduced adhesion also allows easier and faster removal of water droplets with chemically active substances dissolved in them from the surface of the coating under the action of gravity. The use of a modified anti-graffiti coating does not reflect negatively on the properties of the entire paint system. The protective system retains its mechanical properties such as hardness. adhesion and scratch resistance. Also, the modified top coat does not negatively affect the protective system's UV-B resistance. condensation moisture resistance and corrosion resistance.

Anti-graffiti coatings used on railway rolling stock are not indestructible and destruction over time. Heavy rainfall, high humidity, extreme temperatures, and aggressive UV radiation can gradually weaken their structure and functional properties. Proper preparation of the substrate before coating application, as well as regular inspections and professional maintenance, can significantly extend the operational life of paint coatings.

Modification of the surface tension of the anti-graffiti coating in the liquid phase prior to application to vehicle surfaces has a very positive effect on its spreadability, which translates into low roughness of the resulting surface layer. Small values of roughness affect the reduction of adhesion forces by reducing the specific surface area contacting the anti-graffiti protective coating with unwanted contaminants.

A very important factor affecting the geometric structure of the coating system is the proper

preparation of the substrate material. Paint systems are characterized by lower roughness in relation to the substrate material (two orders of magnitude). In addition, the isometric images of the coating systems show traces of the preceding treatment, which was sanding.

The XPC 60011 anti-graffiti coating system has the highest adhesion, while the XPC 60012 paint system has the lowest adhesion.

The BO100-AGR anti-graffiti coating system has similar mechanical properties with respect to the anti-graffiti coating systems of a foreign manufacturer (PPG).

Economic considerations and environmental requirements make it necessary to introduce new solutions that ensure a reduction in unit manufacturing costs while ensuring the quality of the produced paint systems. The physical properties of the surface layer are important due to the stability of the technological process using the phenomenon of adhesion.

A multifaceted approach to counteract the formation of graffiti on railroad cars requires the following measures:

- Investment in equipping the rail base with a system of monitoring and protection of railroads using modern technologies;
- Organization of preventive measures in the form of patrols specializing in chasing graffiti artists during the day;
- Organization of security services including night patrols with the use of advanced technologies including surprise actions involving the organization of so-called "ambushes" in places where railway depots spend the night;
- Widespread implementation of the procedure for identifying and removing graffiti from railroad cars especially in the context of removing the graffiti coating as soon as possible.

## CONCLUSIONS

Based on the conducted experiments and analysis of the obtained test results of anti-graffiti coating systems, the following conclusions can be drawn:

1. Railway companies need protection systems for their vehicles and wagons.
2. The BO100-AGR anti-graffiti coating system was characterized by similar mechanical properties to the anti-graffiti coating systems of a foreign manufacturer (PPG).
3. The analysis of the microstructure showed that the thickness of the anti-graffiti coating systems was in the range of 2300–2400 μm. Moreover, the paint systems were free of pores and micro-cracks.
4. The BO100-AGR anti-graffiti coating system had the lowest free surface energy. Compared to the other three anti-graffiti coating systems, the BO100-AGR paint system had the best anti-adhesive properties. The anti-adhesive properties of the BO100-AGR system may be of great importance in a potential application on rail vehicles.
5. Economic considerations make it necessary to introduce new solutions that ensure the reduction of unit manufacturing costs while ensuring the quality of the produced paint systems. The physical properties of the surface layer are important due to the stability of the technological process using the phenomenon of adhesion.
6. It is necessary to strictly maintain quality requirements both in the preparation of anti-graffiti coatings and in their removal.
7. The use of anti-graffiti coatings reduces the negative impact on the environment with a view to reducing the negative impact on the ecosystem.
8. An alternative method of vehicle skin protection that is currently possible is to cover vehicles with a special film, which significantly increases anti-graffiti protection. According to the manufacturer's declaration, the special film guarantees a seven-year warranty on the material, as well as no limit on the number of graffiti removals when using dedicated agents for this process.

## REFERENCES

1. Vega-Bosh A., Santamarina-Campos V., Bosh-Roig P. Assessing the feasibility of removing graffiti from railway vehicles using ultra-freezing air projection. Appl Sci. 2024;14(10):4165. https://doi.org/10.3390/app14104165
2. Pietrzak A., Ulewicz M., Kozień E., Pietraszek J. Application of a mixture of fly ash and solid waste from gas treatment from municipal solid waste incineration in cement mortar. Materials. 2025;18:481. https://doi.org/10.3390/ma18030481
3. https://www.skm.warszawa.pl/mozna-poradzic-sobie-z-graffiti-choc-to-walka-nie-tylko-ze-spreyowcami-ale-takze-silna-konkurencja-pomiedzy-producentami-farb-i-powlok-antygraffiti-od-lat-tocza-miedzy-soba-

wojne-o-zwyciestwo-a-za-2/ (accessed on 15.06.2025)

4. https://lovekrakow.pl/aktualnosci/malopolska-zamawia-nowe-pociagi-z-powloka-antygraffiti_33921.html (accessed on 15.06.2025)
5. Pasieczyński Ł. Performance properties of anti-graffiti coating systems for railway rolling stock. PhD Dissertation, Kielce: Kielce University of Technology, Poland; 2019. (in Polish)
6. Radek N. Properties of WC-Co coatings with $Al_2O_3$ addition. Production Engineering Archives. 2023;29(1):94-100. https://doi.org/10.30657/pea.2023.29.11
7. Burakowski T. Areology - theoretical foundations. Radom: Scientific Publishing
8. House of the Institute for Sustainable Technologies - National Research Institute; 2013. (in Polish)
9. Batchelor A.W., Stachowiak G.W. Predicting synergism between corrosion and abrasive wear. Wear. 1988;123:281–291. https://doi.org/10.1016/0043-1648(88)90144-5
10. Radek N., et al. Operational tests of coating systems in military technology applications. Eksploatacja i Niezawodność - Maintenance and Reliability. 2023;25(1):1–13. https://doi.org/10.17531/ein.2023.1.12
11. Decker C., Balandier M. Degradation of poli(vinyl chloride) by U.V. radiation - I. Kinetics and quantum yields. European Polymer Journal. 1982;18:1085–1091. https://doi.org/10.1016/0014-3057(82)90209-9
12. Decker C., Biry S. Light stabilization of polymers by radiation-cured acrylic coatings. Progress in Organic Coatings. 1996;29(1–4):81–87. https://doi.org/10.1016/S0300-9440(96)00630-3
13. Kotnarowska D. Influence of ultraviolet radiation on erosive resistance of modified epoxy coatings. Solid State Phenomena. 2006;113:585–588. https://doi.org/10.4028/www.scientific.net/SSP.113.583
14. Kotnarowska D. Analysis of polyurethane top-coat destruction influence on erosion kinetics of polyurethane-epoxy coating system. Eksploatacja i Niezawodność - Maintenance and Reliability. 2019;21(1):103–114. http://doi.org/10.17531/ein.2019.1.12
15. Kotnarowska, D. Influence of ultraviolet radiation and aggressive media on epoxy coating degradation. Progress in Organic Coatings. 1999;37(3–4):149–159. http://doi.org/10.1016/S0300-9440(99)00070-3
16. Kazicyna L.A., Kupletska N.B. Spectroscopic methods for determining the structure of organic compounds. Warsaw: PWN; 1976. (in Polish)
17. Dobrzański L. Fundamentals of materials science and metallurgy. Warsaw: WNT; 2002. (in Polish)
18. Nguyen T., Bentz D., Byrd E. Method for measuring water diffusion in a coating applied to a substrate. Journal of Coatings Technology. 1995;67(844):37–46.
19. Nguyen T., Hubbard J.B., Pommersheim J.M. Unified model for the degradation of organic coatings on steel in a neutral electrolyte. Journal of Coatings Technology. 1996;68(855):45–56.
20. Sokólski W. World Corrosion Organization – origins, mission and goals, program of action. Ochrona przed korozją. 2009;52(9):1–4. (in Polish)
21. Kotnarowska D. Destruction of Epoxy Coatings under the Influence of Sodium Chloride Water Solutions. Solid State Phenomena. 2015;220–221:609–614. http://doi.org/10.4028/www.scientific.net/SSP.220-221.609
22. Kohl M., Kalendova A. Anticorrosion properties of organic coatings containing polyphenylenediamine phosphate. Advances in Sciences and Technology Research Journal. 2015;9(29):47–50. http://doi.org/10.12913/22998624/60782
23. Mróz A., Szymański M., Koch P., Pawlicki M., Meller A., Przekop R.E. The influence of surface texture of elements made of PA6-based composites on anti-graffiti effect of paint coating. Materials. 2024;17(9):1951. https://doi.org/10.3390/ma17091951
24. Bartman M., Balicki S., Wilk K.A. Formulation of environmentally safe graffiti remover containing esterified plant oils and sugar surfactant. Molecules. 2021;26:4706. https://doi.org/10.3390/molecules26154706
25. Amrutkar S., More A., Mestry S., Mhaske S.T. Recent developments in the anti-graffiti coatings: an attentive review. Journal of Coatings Technology and Research. 2022;19:717–739. https://doi.org/10.1007/s11998-021-00580-z
26. Gao P., Wang Y., Wang H., Wang J., Men X., Zhang Z., Lu Y. Liquid-like transparent and flexible coatings for anti-graffiti applications. Progress in Organic Coatings. 2021;161:106476. https://doi.org/10.1016/j.porgcoat.2021.106476
27. Berscha J.D., Flores-Colena I., Masuero A.B., Molin D. An overview of the efficiency of anti-graffiti products in the context of climate change. Procedia Structural Integrity. 2024;55:57–63. https://doi.org/*10.1016/j.prostr.2024.02.008*
28. https://wiadomosci.wp.pl/graffiti-kosztowny-wandalizm-6109012257666177a (accessed on 15.06.2025).
29. https://zbiorowy.info/2018/11/jak-przewoznicy-radza-sobie-z-wandalizmem/ (accessed on 15.06.2025)
30. https://kurier-kolejowy.pl/aktualnosci/41870/wandalizm-graffiti-na-pociagach-renfe-wygenerowal-koszty-w-wysokosci-ponad-25-milionow-euro.html (accessed on 15.06.2025)

31. https://haloursynow.pl/pl/11_wiadomosci/784_stolica/21767_akt-wandalizmu-sparalizowal-metro-zaciagneli-hamulec.html (accessed on 15.06.2025)
32. https://www.fakt.pl/wydarzenia/polska/warszawa/groza-w-warszawskim-metrze-zatrzymali-pociag-pasazerowie-byli-przerazeni/x1pr6hl (accessed on 15.06.2025)
33. https://www.fakt.pl/wydarzenia/polska/warszawa/szokujace-sceny-z-warszawskiego-metra-nikt-nie-przeszkodzil-wandalom/qqcve5k (accessed on 15.06.2025)
34. Radek N., Pasieczyński Ł., Pietraszek J., Broncek J. Analysis of the surface geometric structure of the anti-graffiti coating systems intended for rolling stock. Mechanik. 2019;2:124–127. https://doi.org/10.17814/mechanik.2019.2.21 (in Polish)
35. Kłonica M. Application of the ozonation process for shaping the energy properties of the surface layer of polymer construction materials. Journal of Ecological Engineering. 2022; 23(2):212–219. https://doi.org/10.12911/22998993/145265
36. Kłonica M., Kuczmaszewski J. Modification of Ti6Al4V titanium alloy surface layer in the ozone atmosphere. Materials. 2019; 12(13): 2113. https://doi.org/10.3390/ma12132113
37. Adamczak S., Makieła W. Analyzing variations in roundness profile parameters during the wavelet decomposition process using the MATLAB environment. Metrology and Measurement Systems. 2011;XVIII(1):25–34.
38. Miller T., Adamczak S., Świderski J., Wieczorowski M., Łętocha A., Gapiński B. Influence of temperature gradient on surface texture measurements with the use of profilometry. Bulletin of the Polish Academy of Sciences. 2017;65(1):53–61. https://doi.org/10.1515/bpasts-2017-0007
39. Oczoś K., Lubimov V. Geometric structure of the surface. Rzeszów: Publishing house of the Rzeszów University of Technology; 2003. (in Polish)
40. PN-EN ISO 1522:2008: Paints and varnishes - Pendulum damping test. (in Polish)